

Chapter 18

The oceans and the world's mean climate

The ultimate aim of regional oceanography is not a description of the oceans in their steady state but an understanding of the changes that occur in them over seasons, years and decades. A full understanding of these aspects, to a level where forecasting the oceanic and atmospheric circulation for months or years ahead becomes a realistic possibility, requires close cooperation between regional oceanography and geophysical fluid dynamics. In fact, it inevitably leads to an approach quite different to the approach taken in the first seventeen chapters of this book, which largely ignored the interaction processes between ocean and atmosphere and treated the ocean as a self-contained system. The last three chapters in this book now look at the nature of the interaction and its consequences. It will be seen that the steady state discussed up to this point provides a logical reference for the discussion; so the seventeen chapters were not wasted. It will also become clear that much more work needs to be done before we can claim to fully understand the interplay between ocean and atmosphere.

In earlier chapters we identified momentum transfer (wind stress), heating and cooling, and evaporation and precipitation as the key mechanisms through which the atmosphere exerts an influence on the ocean. We now adopt the opposite point of view and ask: What are the mechanisms through which the ocean exerts an influence on the atmosphere, and hence on the world's climate?

The ocean, evidently, is the dominant source of atmospheric moisture; and the latent heat released when this moisture condenses into rain or snow is the primary driving force for the atmospheric circulation (the global wind systems). The winds in turn affect the sea surface temperature in several different ways; and the sea surface temperature largely controls the magnitude and spatial distribution of the moisture flux to the atmosphere. This shows that the most important oceanic parameter for the atmosphere which provides the link between two components of a tightly coupled system is the sea surface temperature (SST). A discussion of the ocean and the world's climate therefore has to begin with a detailed understanding of the SST distribution.

A first and very elementary solution to the problem of understanding SST can be obtained by treating the ocean as a "swamp", i.e. a layer of water so thin that it can store no heat, so the heat budget is balanced locally without assistance from currents. In a "swamp" ocean, the net heat flux into the ocean at any locality is exactly zero at all times. This assumption allows an easy estimate of SST from which evaporation into the atmosphere may be estimated. The resulting "swamp temperature" (known as the equilibrium temperature, Figure 18.1) matches reality to the extent that the ocean is warm at the equator and in summer, and cold at the poles and in winter. It is quite a useful first guess against which to measure the effects of ocean currents on SST; but it cannot explain the observation that seasonal temperature variations are much larger over land than over sea. SST varies by little more than 30°C, from -2°C near the poles to 30°C in the equatorial Pacific Ocean; at any particular location its daily variation rarely exceeds 1°C, and its difference between winter and summer usually falls within $\pm 5^\circ\text{C}$. In contrast, surface temperatures over land can vary by as much as 100°C over the earth's surface; the daily temperature range exceeds 10°C in many places, and the difference between summer and winter temperatures comes close to 100°C in extreme continental climates.

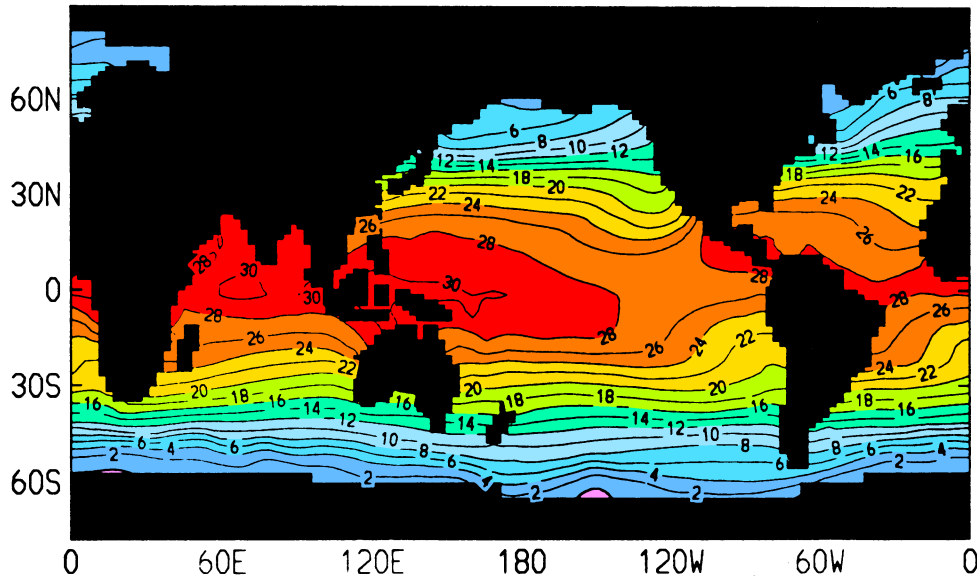


Fig. 18.1. Annual mean equilibrium surface temperature ($^{\circ}\text{C}$) for the world ocean. This is the temperature the sea surface would have if the heat budget were locally balanced at all times. Note the similarity with the observed annual mean surface temperature (Fig. 2.5a) but also the differences in regions of strong currents and upwelling. From Hirst and Godfrey (1992).

A somewhat better approximation to this situation is to treat the ocean as a passive “slab”, perhaps 100 m deep, i.e. to allow it to absorb heat during summer and release it again in winter, through the formation of the seasonal mixed layer (Chapter 5). Relative to the atmosphere, the storage capacity of the ocean for heat is huge (about 1000 kcal are released by every 3100 m^3 of dry air or 1 m^3 of sea water if their temperature is lowered by 1°C). This results in a seasonal SST cycle almost three months out of phase with the solar heating and much reduced in amplitude compared to that found in places far from the sea. Thus heat storage in the mixed layer results in milder climates for coastal and island locations, and a slab model can reproduce these effects quite well.

However, both the swamp and slab models are very deficient for representing the earth's mean climate, particularly if one wishes to understand its year-to-year variations. The ocean can and does absorb heat in one region, carry the heated water below the surface by subduction (Figure 5.3) or deep convection, and return the heat to the atmosphere many thousands of kilometers away and years, decades or even centuries later. In the mean, this results in the transport of heat from the equator towards the poles, tending to cool the tropics and heat the polar regions; the efficiency of this process is comparable to that of the atmosphere (Figure 18.2). The difference is that this process is carried out by ocean currents with a cycle time of many years. The strength of these currents varies, so we can expect year-to-year variations of the heat exchange with the atmosphere. To give two examples, the big region of heat gain in the eastern equatorial Pacific seen in Figure 1.6 largely disappears in some years (known as El Niño years, discussed in Chapter 19), with drastic effects on the world's climate; and there are reasons to suspect that the region of heat

loss in the far north Atlantic Ocean may vary substantially from decade to decade (see Chapter 20). Climatologists believe that these year-to-year variations of the heat exchange with the atmosphere are a major contributor to the observed natural variations of climate.

Similarly, long-term mean evaporation in one part of the ocean produces a continuous supply of salty water, which must be carried to some other part where there is an excess of rainfall or runoff. Once again, the transport can take many years to accomplish and is subject to interannual changes. These, too, may have effects on climate, as will be discussed in Chapter 20.

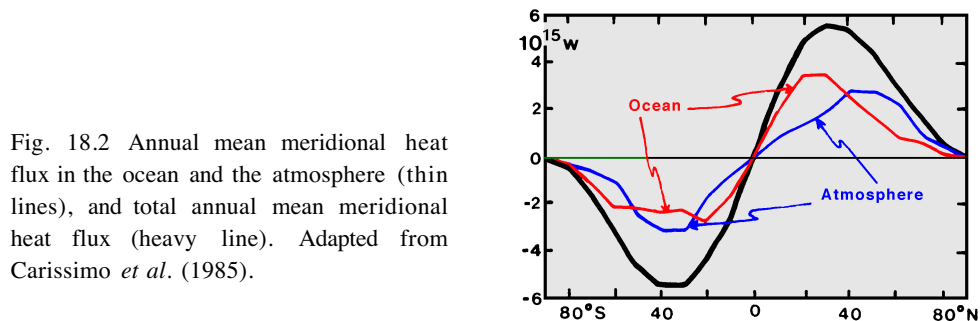


Fig. 18.2 Annual mean meridional heat flux in the ocean and the atmosphere (thin lines), and total annual mean meridional heat flux (heavy line). Adapted from Carissimo *et al.* (1985).

In this chapter we shall review what we know about the long-term mean surface fluxes of heat and moisture and about how the ocean currents are organized to transport heat and freshwater from where it is absorbed to where it is released. We will rely strongly on descriptions given in earlier chapters. However, our data base does not yet allow us to draw solid inferences about future climate trends, and some recourse to theoretical modelling of the climate system is necessary even in a text on regional - i.e. observational - oceanography. Numerical modellers have made considerable progress in creating realistic models of the ocean circulation in recent years, and these models allow us to explore the potential of the ocean as an active agent in the world's climate. One of their main results is that the atmosphere is particularly sensitive to small changes in sea surface temperature in the tropics; the reasons for this are discussed in the final section of this chapter, in the context of the mean seasonal *atmospheric* circulation. This information is needed in the last two chapters, where we discuss how the coupled ocean-atmosphere system operates to generate year-to-year and longer term climate variations.

Observed heat fluxes into the ocean

As mentioned in Chapter 1, it is quite difficult to estimate the net heat flux into the ocean accurately, because it is typically a small residual of four terms, two of which are relatively large and not very well determined by observations. *Solar heating* is nearly always the largest contributor, tending to warm the ocean surface. Simple rules have been

devised for estimating the flux of solar radiation into the ocean from data on cloud cover, which have been collected by merchant ship's officers; world maps of solar (or "short-wave") radiation entering the ocean (such as Figure 1.5) are essentially maps of merchant ship cloud cover estimates, modulated by the geographic variation of clear-sky radiation (which is simply a function of latitude and season). Even with "perfect" cloud data, different algorithms (known as bulk formulae) differ in their estimates of the net solar radiation by about 10 - 20% (e.g. Hanawa and Kizu, 1990). Evaporation cools the ocean surface and is responsible for the second most important term in the heat budget, *latent heat loss* (Figure 18.3), particularly in the tropics. It can be estimated from other simple rules, using data on wind speed, the "wet bulb" and "dry bulb" temperatures, and sea surface temperature, all of which are also routinely collected by merchant ship officers. Again, different algorithms can yield results that differ by as much as 30 W m^{-2} (Godfrey *et al.*, 1991; 30 W m^{-2} is enough to warm a layer of water 50 m thick by 0.5°C per month).

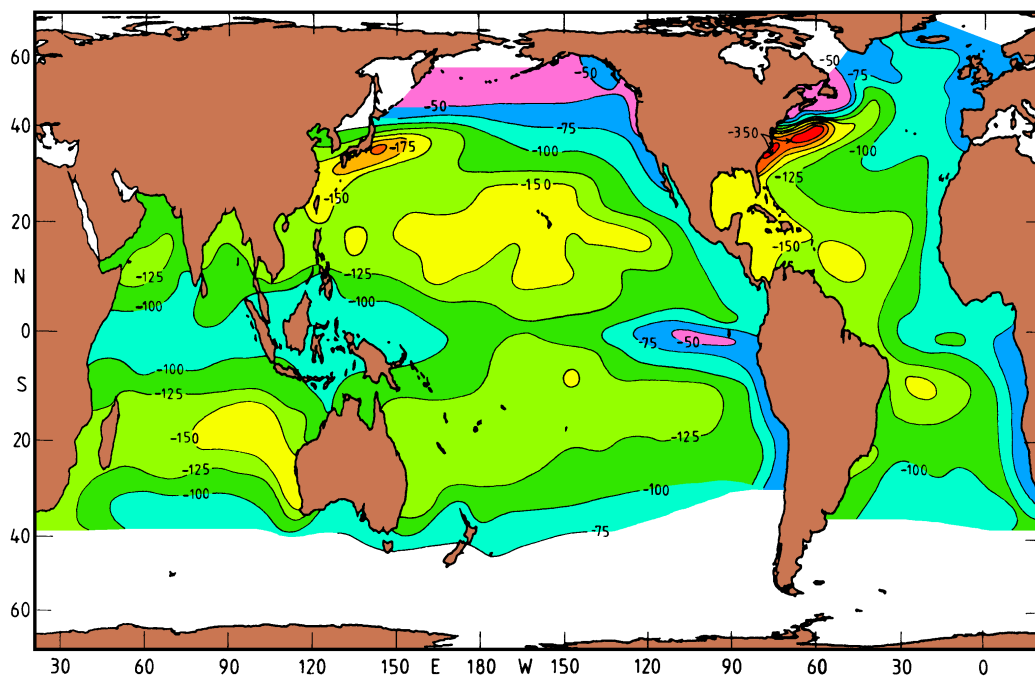


Fig. 18.3. Annual mean latent heat flux (W m^{-2}). Oceanic heat loss to the atmosphere is shown as negative numbers. From Oberhuber (1988).

Two other types of heat flux - *sensible heat transfer* (the direct, mechanical transfer of heat between air and water when the two media have different temperatures) and *net longwave radiation* (the net escape of thermal radiation from the ocean surface) - contribute to the total heat flux; they are generally smaller than the first two but not small enough to be neglected. These also can be estimated from simple rules, using the same merchant ship

data. The net heat flux is found by adding all four contributions. Figure 1.6 shows one such estimate, which was calculated using a particular set of bulk formulae. Other global or regional climatological maps use different bulk formulae or evaluate the fluxes over different time intervals and therefore come to somewhat different conclusions.

The sum of the four contributions is generally only a few tens of W m^{-2} over most parts of the ocean, whereas the rules used for estimating the two largest terms - the solar radiation and latent heat loss - have errors of this order of magnitude; the merchant ship data also contain errors. Furthermore, different techniques are used in averaging the data, which can lead to different smoothing of maxima. This (rather than the different choice of sampling times) is probably the main reason why different climatologies show fairly large differences from region to region. Nevertheless, all climatologies are qualitatively quite similar; and as has already been foreshadowed in earlier chapters, a quite plausible explanation of their general pattern can be given in terms of observed ocean currents. The fact that this is so is a tribute to the care and diligence which merchant ship officers have put into the accurate recording of data over the last hundred years or so, without direct reward to them during their lifetime. Oceanographers and climatologists owe a great debt to them.

Figure 1.6 is an annual mean picture of the ocean heat flux. However, the seasonal cycle in the ocean currents and temperatures both have large amplitudes in many parts of the world. One might therefore expect that it would be necessary to examine the heat budget season by season and then average the result, in order to understand how the ocean achieves the annual mean horizontal transports of heat implied by Figure 1.6. Surprisingly, this does not seem to be so, at least to the limited accuracy of Figure 1.6; one can understand many features of the annual mean heat flux maps quite well in terms of the annual mean currents (provided care is exercised in interpreting the results), and the mean currents are primarily driven by the mean wind stress field. Therefore we will mainly interpret the annual mean heat flux maps, region by region, with annual mean wind stresses and currents. We will discuss reasons why this approach is reasonable at the end of this chapter.

East Pacific and Atlantic upwelling regions

Along the eastern boundaries of the Pacific and Atlantic Oceans, Figure 1.6 shows narrow regions of oceanic heat gain extending from about 50°N to 50°S in the Pacific and from about 50°N to the Cape of Good Hope at 32°S in the Atlantic Ocean. These latitude limits are not very well defined, because of data limitations and the uncertainty in net heat flux estimates discussed above, but they are fairly similar to the points at which the annual mean westerly wind stresses bifurcate at the coast (Figure 1.4a). For example, the westerlies bifurcate at about 44°N in the north Pacific and Atlantic Oceans, near Oregon and northern Spain respectively, and at about 48°S in the South Pacific Ocean. equatorward of these points the nearshore wind stress blows towards the equator everywhere. Upwelling of cold subsurface water is to be expected at the coast, to supply the offshore Ekman drift (Figures 4.1 and 8.25). The associated current systems have been described in Chapters 8 and 14 (Figures 8.26, 8.27, 14.16 and 14.17); the surface currents are equatorward, which also tends to bring in cooler water from higher latitudes and further reduce surface temperature.

If air temperature and humidity, wind speed and cloud cover are all regarded as fixed, a reduction of SST reduces the latent and sensible heat loss, and also the net heat loss by longwave radiation, typically by a total of some 35 W m^{-2} per $^{\circ}\text{C}$ of SST change.

Upwelling typically produces several degrees of cooling. The large net heat flux into the ocean in coastal upwelling regions is thus readily understood.

Coastal upwelling occurs only in the first few tens of kilometers from the coast, whereas the coastal bands of heat gain in Figure 1.6 are as much as a thousand kilometers or more in width, so coastal upwelling by itself does not explain the existence of these bands of heat flux into the ocean. However, the heat capacity of the surface mixed layer is so great that the upwelled water takes several months to warm to the equilibrium temperature; during these months the water can move 1000 km or so offshore with the Ekman drift. Furthermore, after the water is upwelled, it flows equatorward with the Sverdrup flow. Consequently the water moves into steadily warmer climates, causing it to continue to warm for substantial periods after it has upwelled. This advective contribution to surface heating is clearly seen by comparing the annual mean SST map (Figure 2.5a) with surface currents (Figures 8.6 and 14.2). In each of the eastern boundary upwelling regions, the surface currents clearly flow from low temperatures towards high.

Equatorial upwelling regions

Strong bands of oceanic heat gain along the equator are found over the entire width of the Atlantic and over the eastern Pacific Oceans; weaker heat gain occurs in the west Pacific Ocean. Comparison with Figure 1.4a shows that there are moderate easterly wind stresses along the equator in both oceans; in relative terms they are strongest on the western side of the Atlantic and in the central Pacific Ocean.

These winds give rise to large poleward Ekman transports on either side of the equator (Figure 4.1). Upwelling occurs to replace the water that is removed by Ekman transport, as discussed in Chapter 8. The upwelled water is in turn supplied by geostrophically balanced flow in the top few hundred meters. A zonal steric height gradient develops to keep these meridional flows in geostrophic balance. (The Coriolis force changes direction across the equator, so the same zonal steric height gradient produces meridional flows of opposite sign on either side of the equator.) This zonal steric height gradient can be seen along the equator in both the Pacific and Atlantic Oceans in Figure 2.8b.

The heat flux maximum in the equatorial Pacific and Atlantic Oceans (Figure 1.6) lies somewhat to the east of the strongest equatorial easterly winds (Figure 1.4a), i.e. to the east of the strongest upwelling. The reason is that the temperature of upwelled water decreases eastwards along the equator, being coldest at the east of each basin. This fact in turn relates to the zonal gradient of steric height along the equator, set up to balance the wind and provide geostrophic inflow. Since steric height is roughly speaking a vertical integral of temperature, the zonal steric height gradient forces near-surface temperatures to be colder at the eastern end of each basin, where the steric height is lower.

As in the case of the eastern boundary heating regions, the width of the equatorial heating region extends about 1000 km on either side of the equator, much wider than the region of actual upwelling. The reason is again the same as in the coastal upwelling regions. After the water upwells it takes several months for it to absorb enough heat to reach thermal equilibrium with the atmosphere, during which time it can travel 1000 km poleward with the Ekman drift.

Two other factors not related to upwelling also influence equatorial SST in the Pacific and Atlantic Oceans. Both are related to current shear. Vertical current shear between the westward surface flow and the eastward flowing Equatorial Undercurrent produces increased

turbulence (Figures 8.8 and 14.4) and assists in lowering SST. Horizontal shear between the South Equatorial Current and the North Equatorial Countercurrent gives rise to wave-like instabilities in the central and eastern Pacific Ocean (Figure 8.14). These waves are believed to transport substantial quantities of heat towards the equator, helping to reduce the intensity of the surface heat flux patch in the eastern Pacific Ocean.

Equatorial Indian Ocean heating regions

The pattern of surface heating in the Indian Ocean is unlike the pattern in the other two major ocean basins. The Indian Ocean is also the one where different climatologies show more significant differences in net surface heat flux than in any other ocean; for example, Figure 1.6 indicates an equatorial heating maximum in the western Indian Ocean, a feature weak or absent in other climatologies. However, all climatologies agree that heating is greatest at the *western* side of the basin - a major difference from the pattern in the Atlantic and Pacific Oceans which requires explanation.

Alongshore winds along the west coast of Indonesia and the east side of the Bay of Bengal do not strongly favour upwelling at any time, except along the coast of Java in the Asian summer monsoon (Figure 1.4b). Furthermore, as discussed in Chapter 11, the vertical temperature gradient is not quite so sharp near the surface as it is in the eastern Atlantic and Pacific Oceans, so more upward motion is needed before surface cooling can be generated. Upwelling does occur along the south Java coast around August, but when the net heat flux is averaged over the year it does not result in an obvious patch of upwelling-induced heat gain like that off the Atlantic and Pacific east coasts. The net result is that heat gain along the eastern side of the Indian Ocean is somewhat weaker than in the other two oceans. By contrast, annual mean winds favour upwelling along the Arabian, east Indian, and east African coasts in the northern hemisphere (Figure 1.4). This upwelling and associated heat gain along the western boundary, a feature unique to the Indian Ocean, primarily occurs during the summer monsoon when intense southwesterlies blow along all these coasts. As in the *eastern* Pacific and Atlantic Oceans, upwelling and horizontal advection are both essential components in generating the broad-scale pattern of heat flux seen in the western equatorial Indian Ocean (McCreary and Kundu, 1989).

As discussed in Chapter 11, the seasonal flow regime that results along the African and Arabian coasts from the monsoon winds is extremely complex, and quite detailed numerical modelling may be necessary even for a rough understanding of the heat budget of the northern Indian Ocean as a whole. Nevertheless, it is worth noting that the annual mean wind stress pattern of Figure 1.4a implies southward Ekman fluxes nearly everywhere north of about 15°S in the Indian Ocean. This must be balanced by an equal and opposite net northward geostrophic flow reaching deeper than the Ekman layer and therefore having an average temperature several degrees lower than that of the surface Ekman drift. The southward heat transport associated with this balanced pair of flows is of the same order of magnitude as the net heat flux through the sea surface (this can be estimated from Figure 1.6 by integrating the fluxes over the Indian Ocean north of 15°S). Thus even in this strongly seasonal region, the amount of heat transported out may be primarily controlled by the annual mean winds.

A notable feature in all climatologies is the region of quite large net heat flux into the ocean in the Indonesian throughflow region. This region does not contain any major upwelling, so the explanation for the large oceanic heat gain must be found somewhere

else. In Chapter 13 it was argued that turbulent mixing must be anomalously strong in Indonesian waters and that its effect must be felt to 1000 m depth. This reduces SST and distributes the heat input from the atmosphere over a deeper "slab" than elsewhere in the world ocean. This is the only equatorial region in the world ocean where large heat gain is achieved without upwelling.

The Leeuwin Current

The zero heat flux contour in Figure 1.6 meets the continents near 50°N and S in the eastern Atlantic and Pacific Oceans but closer to 20°S in the Indian Ocean. This major difference between the ocean basins does not reflect a difference in the wind regime (Figure 1.4a) but a difference in the details of the eastern boundary regime. As discussed in Chapter 11, the upwelling that one might expect from the equatorward winds between 20° and 34°S along the western Australian coast is overwhelmed by an onshore geostrophic drift. The meridional pressure gradient needed to maintain the onshore drift is supplied by heat loss near Western Australia (clearly seen in Fig 1.6) which cools water at the southern end of the continent, reducing steric height from the very high levels found off northwestern Australia. This is one rare instance in which the currents carrying heat fluxes in the ocean are created by the heat fluxes themselves, i.e. by thermohaline processes; most surface currents are driven by wind forcing. However, as remarked in Chapter 11, the whole Leeuwin Current system can be regarded as being driven by winds along the equatorial Pacific Ocean, which pile up warm water in the west Pacific region and hence bring very warm water to northwestern Australia.

The subtropical western boundaries

One feature which emerges clearly from Figure 1.6 is that the Kuroshio and Gulf Stream and its extensions release massive amounts of heat to the atmosphere. This occurs mainly in winter when cold winds blow from Siberia and Canada respectively across the warm, poleward flowing waters of these currents; heat loss during summer is low and may turn into heat gain on occasions. On annual average, however, heat is lost from the ocean in the western boundary currents and extension regions. This heat loss results in convective sinking of surface water, so the extension regions of western boundary currents in the northern hemisphere are important regions for water mass formation. The subtropical mode waters have their origin in these regions, from where they are subducted into the subtropical gyres of the north Pacific and Atlantic Oceans.

By contrast, the heat losses from the western boundary currents of the Southern Hemisphere seem very small. In the case of the Brazil and East Australian Currents data are probably quite adequate to yield reasonable heat flux estimates, so that the small heat losses associated with these two currents are probably valid. Furthermore, the result is not unexpected. First, both currents are quite weak, the Brazil Current because it is opposed by the thermal flow towards the north Atlantic Ocean and the East Australian Current because a substantial fraction of its potential transport is drained away by the Indonesian throughflow. Secondly, no analogue of the very cold and dry Canadian and Siberian winter winds blow over either of these two currents.

The apparent weakness of the heat loss from the Agulhas Current and its extension suggested by Figure 1.6 is harder to understand and may be an artifact of the climatology.

The Agulhas Current is among the strongest western boundary currents in the world ocean and experiences heat loss in all seasons (Chapter 11). It may be that the observational data used to construct Figure 1.6 are inadequate in the Agulhas Current region; the same is probably true for the western boundary current along New Zealand and its extension.

The subpolar north Atlantic Ocean

A region of heat loss without analogue in the other ocean basins can be seen in the subpolar north Atlantic Ocean. A remarkable aspect of the heat budget in that region is that the ocean currents supplying the surface heat flux are generated to some degree by the heat fluxes themselves, i.e. driven to some degree by thermohaline forcing and not by the wind stress alone. The situation is somewhat similar to that of the Leeuwin Current, but in the north Atlantic Ocean the process is strongly modulated by salinity effects.

It has already been remarked in Chapter 15 that the north Atlantic is substantially saltier than the north Pacific Ocean. Part of the reason for this is that much of the freshwater evaporated from the north Atlantic Ocean is carried over the low mountain ranges of Central America by the Trade Winds and rains out near the terminus of the Pacific North Equatorial Countercurrent. (This is the major reason for the large difference in *P-E* in the Atlantic relative to the Pacific Ocean seen in Figure 1.7). The freshened water in the Pacific Ocean is carried northward into the north Pacific subtropical gyre. Meanwhile the saltier water in the north Atlantic Ocean enters the Gulf Stream and moves northward. Another contribution is thought to come from the Agulhas Current eddies, which carry salt from the Indian into the Atlantic Ocean.

This saltiness of north Atlantic surface water has an important consequence. The salty subtropical water flows northeastward across the Atlantic to the Arctic Ocean in the North Atlantic and Norwegian Currents; it moves fast enough that the net positive *P-E* in the temperate north Atlantic Ocean (Figure 1.7) is not able to freshen this water greatly, so it remains very salty (relative to the north Pacific Ocean) at 60° - 70°N. As was discussed in connection with the formation of North Atlantic Deep Water in Chapter 7, the presence of this high salinity water below the surface water in the Greenland Sea means that little cooling is required to start convective overturn and sinking. This process of North Atlantic Deep Water formation has a self-perpetuating character. Because the water moves through the temperate north Atlantic Ocean so fast it remains salty despite freshwater input into the region and therefore sinks after cooling; in doing so, it pulls more water along behind it, maintaining the rapid flow in the surface layer. The rate of North Atlantic Deep Water formation was estimated in Chapter 7 at about 15 Sv. To put it another way, about 1300 cubic kilometers of water sink from the surface of the north Atlantic Ocean to several thousand meters depth every day, to return southward as North Atlantic Deep Water. If this water is supplied from the upper 500 m of the ocean, this corresponds to an ocean region of 50 km side length - the area of Los Angeles or Greater Tokyo. Not surprisingly, the cooling of this much water from temperatures near 12 - 15°C down to 0 - 4°C implies a major warming of the atmosphere; it is thought to be the reason why northwestern Europe is so markedly warmer than western Canada and Alaska at the same latitudes — water in the upper 500 m there is much too fresh to permit the formation of Deep Water in the north Pacific Ocean.

This process illustrates the subtle nature of the dependence of the earth's climate on apparently minor topographic detail. Central America forms a complete blockage of the

Pacific from the Atlantic Ocean; yet it is low enough to permit moisture transport across it in the atmosphere, so that the north Atlantic Ocean becomes salty while the north Pacific Ocean becomes fresh. One may therefore say that northwestern Europe is warmer than Canada and Alaska because there is a low but complete land blockage in Central America.

The global freshwater and salt budgets

As noted earlier, estimates of precipitation and evaporation over the ocean (Figure 1.7) are subject to even greater uncertainties than the net heat flux field. Consequently we will not discuss the freshwater and salt budgets nearly as fully as the heat budget. We begin by noting two things. Firstly, it is evident from our earlier considerations on the transport of heat at the end of Chapter 4 that a net transport of salt or of freshwater can exist even if the net mass transport is zero. Secondly, salt and freshwater can both be transported in the same direction. This fact is somewhat contrary to intuition, since one might think that relative to the oceanic mean, freshwater is negative salt load and should therefore always be flowing in a direction opposite to the direction of the salt flux (readers familiar with estuarine oceanography will recognize this concept). Figure 18.4 shows that this is not so when the $P - E$ difference becomes a major contribution to the budget. The two quantities are then no longer inversely related.

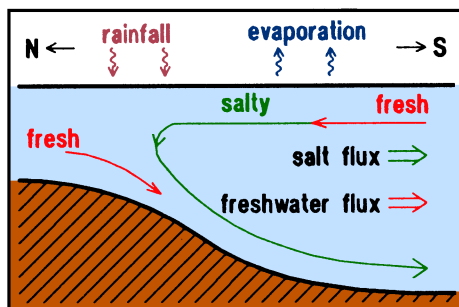


Fig. 18.4. A sketch of salt and freshwater transport in an ocean basin resembling the north Atlantic Ocean. At the surface, water gets saltier as it moves from the tropics through the subpolar gyre to the region where it sinks to carry salt southward in the deeper layers; this produces southward salt transport. Freshwater is imported from the Arctic Mediterranean Sea, in quantities not sufficient to lower the salinity in the deeper layer beyond the tropical surface salinities; while it therefore does not reverse the salt flux, it traverses the ocean from north to south, producing a freshwater flux in the same direction as the salt flux.

Considering these two facts it turns out that an accurate estimate of the transport through Bering Strait is very important for the correct determination of both the salt and freshwater fluxes. In the discussion of the Arctic Mediterranean Sea (Chapter 7) we argued that mass transport through Bering Strait is less than 1 Sv and can be neglected in the global mass budget; in other words, in any model of the global oceanic circulation Bering Strait could

be considered closed. For many years it was taken for granted that the same simplification could be applied in a model of the global salt and freshwater budgets. Such a model produces a net southward transport of salt for the north Atlantic Ocean, as a consequence of high evaporation in the North Atlantic Current and Deep Water formation and return flow (Figure 18.4), and a northward freshwater transport that decreases from large values in the

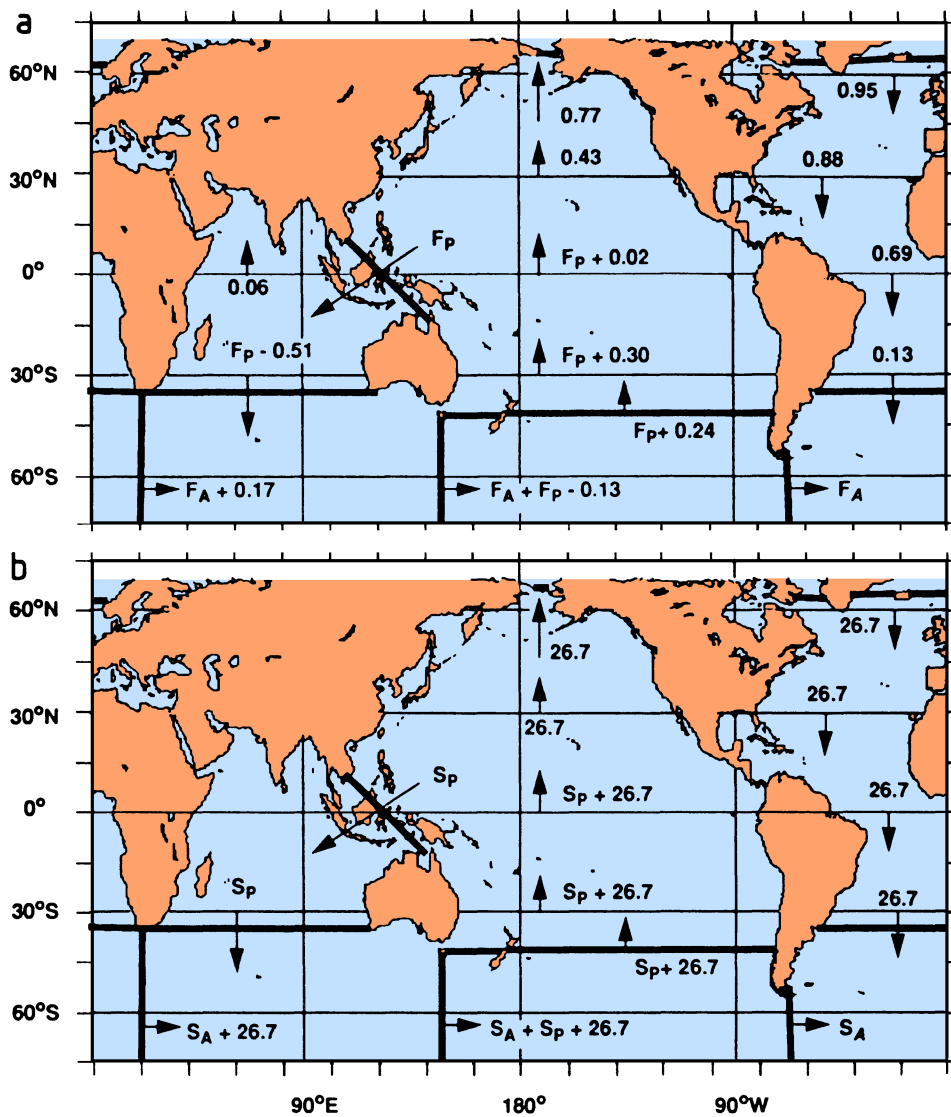


Fig. 18.5. Transports of (a) freshwater (10^9 kg s^{-1}) and (b) salt (10^6 kg s^{-1}) by the oceans, relative to the (undetermined) transports through the passages around Antarctica (index A) and in the Indonesian throughflow (index P). From Wijffels *et al.* (1991).

south Atlantic Ocean to zero in the Arctic Mediterranean Sea. Wijffels *et al.* (1991) pointed out only recently that the surface salinities of the north Pacific Ocean are so low (near 32, see Figure 2.5b) that their freshwater content relative to the global mean salinity is of order 10%. In their budget calculations they use 1.5 Sv for the flow through Bering Strait; this produces a freshwater transport of $150,000 \text{ m}^3 \text{ s}^{-1}$, several times the mean flow of the Amazon River! Thus the Bering Strait throughflow is a major contributor to the world freshwater balance, and if it is accounted for, freshwater transport in the Atlantic Ocean is southward everywhere. Figure 18.5 shows the resulting global flux distribution for salt and freshwater. Note that unlike freshwater, salt does not escape through the sea surface, so the salt transport is the same in each of the major subdivisions of the world ocean.

This discussion illustrates why the north Pacific becomes so much fresher than the north Atlantic Ocean. One can imagine that if the two basins were suddenly forced to have equal salinities, Deep Water might form in both; but to maintain this state of affairs it would be necessary to increase the Central American land barrier sufficiently in order to suppress the flux of moisture from the Atlantic to the Pacific Ocean. With the present topography of Central America and rainfall distribution the surface salinity of the north Atlantic Ocean would gradually increase, while the surface salinity of the north Pacific Ocean would decrease, enhancing Deep Water formation in the Atlantic and retarding it in the Pacific Ocean. Pacific Deep Water formation would eventually cease, and near-surface salinities would continue to decrease in the north Pacific Ocean until they became so low that the small Bering Strait throughflow could drain off a freshwater flux equal to the flux over Central America. It is interesting to speculate what the surface salinity in the north Pacific Ocean must have been during the last Ice Age, when the Bering Strait was blocked.

Model heat flux patterns in the Southern Ocean

The discussion of the last few paragraphs carried us to the limits of what we can achieve with today's data set. Global budgets require global data coverage, which is difficult to achieve even with modern means. Satellites will make a major contribution here, at least for the global heat budget. But we are still desperately short of data particularly in the Southern Ocean (which is a major unknown in Figure 18.5). Recourse to numerical modelling is therefore essential if we want to learn more about the climate without waiting for many more years until the needed data arrive.

Numerical models of the oceanic circulation have the advantage that they do not depend on the details of the heat and evaporation algorithms used in generating Figs. 1.6 and 1.7; their estimates of the net surface heat flux depend only on the velocity, temperature and salinity fields of the model itself. Furthermore, most models force surface temperature and salinity (the best known observational parameters) to stay close to observed patterns. Their usefulness for predicting heat and freshwater fluxes therefore depends mainly on their skill in getting the ocean currents correct. In this section we will compare the surface heat flux field from one such model with the observations of Figures 1.6 and 1.7. The model heat flux field turns out to be in reasonable agreement with observations, over the region where data are adequate; similar results are found in a number of other ocean models. Hence it is reasonable to use such models to give us some ideas on the heat flux pattern in the Southern Ocean, where data are not adequate.

The model used here, like several other models, is driven by the observed wind stresses. Furthermore, and again like many other models, it uses the condition that the surface heat flux at each location is proportional to the departure of model SST from some climatological estimate of mean sea surface temperature (e.g. Figure 2.5a). Similarly, $P-E$ is assumed proportional to the departure of model SSS from some climatological observed SSS (e.g. Figure 2.5b). For climate studies such models are run for several thousand simulation years until the model ocean changes so slowly in time that it can reasonably be treated as being in equilibrium. In the model discussed here, the global mean heat flux into the ocean was balanced to within 0.02 W m^{-2} .

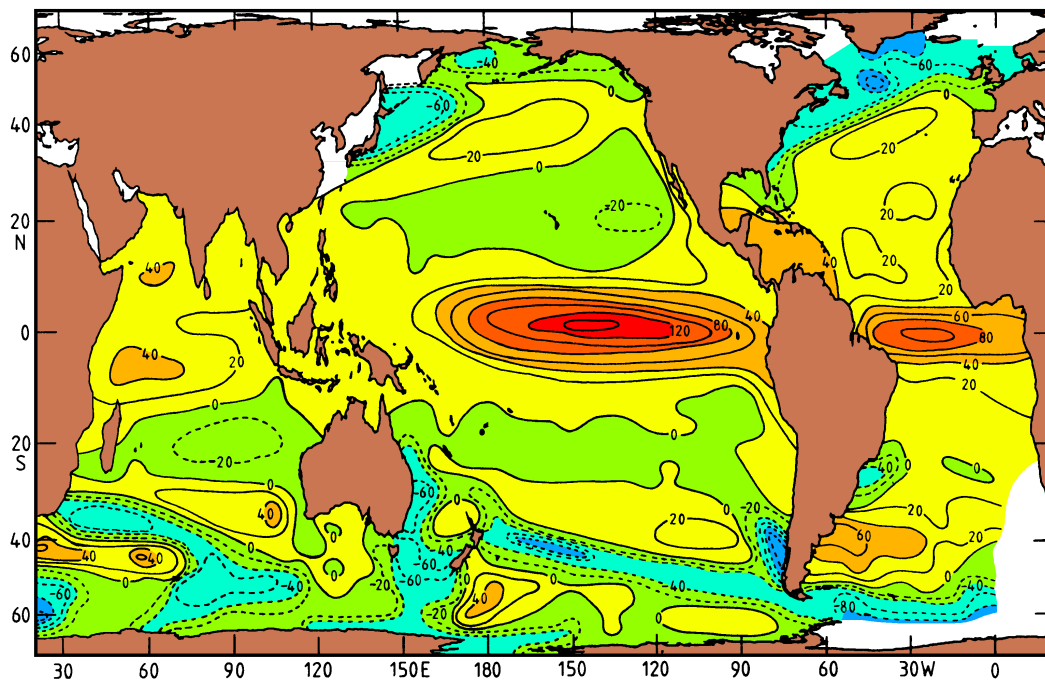


Fig. 18.6. An example of model-derived heat flux (W m^{-2}). After Hirst and Godfrey (1992).

In this equilibrium solution, the current field which develops is primarily set by the surface wind distribution. The winds control the Ekman flow, including the Ekman pumping from the surface layer, and influence the geostrophic flow underneath (through the Sverdrup relation). They also control horizontal variations of the depth-integrated steric height, as discussed in Chapter 4; these are set by the requirement to hold the Sverdrup flow in geostrophic balance. Thermal effects are also important; they control the mean depth of the thermocline (and hence the magnitude and vertical extent of typical surface geostrophic currents), and they also result in some examples of density driven flows roughly where we expect them to occur, on the basis of discussions earlier in this chapter.

Figure 18.6 shows the model's equilibrium heat flux distribution for the world ocean. The observed heat flux pattern (Figure 1.6) is generally reproduced by the model. The heat flux at the eastern Pacific and Atlantic boundaries is not as large as in the observations, but the model ocean gains heat near the coast from at least 40°S to 50°N in the Pacific, and from the Cape of Good Hope to Spain in the Atlantic Ocean. By contrast, heat is lost from the model ocean off western Australia south of 20°S, again in agreement with observations. No heat flux maximum is found in Indonesia because no allowance was made for enhanced vertical mixing in this region. As the model is driven only by annual mean wind stresses, the model heat flux in the western Indian Ocean comes out somewhat smaller than the observed annual mean. Strong heat fluxes out of the ocean occur in the Kuroshio and the Gulf Stream, and weak heat fluxes out of the ocean occur in the Brazil Current and the East Australian Current. All these features are qualitatively much the same as in the observations. Since the forcing of this model contains no seasonal cycle, its broad agreement with reality provides one reason for believing that much of the net heat flux into the ocean is controlled by the annual mean currents.

The similarities between model and observations encourage us to tentatively interpret the model heat fluxes in data-poor regions, as if they were real. It is worth examining the nature of the model surface heat budget in some detail for the Southern Ocean, because the results of this and other models provide the most reliable guide so far as to the nature of heat exchange processes in this very important part of the ocean.

It is evident from Figure 18.6 that two large bands of heat loss from the ocean occur in the model Southern Ocean, stretching eastward and slightly southward from the Agulhas retroflexion and from New Zealand. This tends to confirm the suspicion that the observations must be missing a large part of the heat loss from the Agulhas and East Australian Current systems, respectively. Support for the value of the model also comes from the fact that the two heat loss bands coincide with observed locations of Subantarctic Mode Water formation (Chapter 6). Heat loss leads to convective overturn, and the model, too, shows deep mixed layers beneath the heat loss bands.

Two distinct bands of oceanic heat gain are seen south of the two heat loss bands. One occurs in the Atlantic and western Indian Ocean, south of the Agulhas Current; the second occurs south of the New Zealand boundary current. In these regions Ekman transports are northward and increase northwards, so that upwelling occurs, and surface water is moved towards warmer climates; both processes will favour heat gain by the ocean. Further south still more heat loss occurs near the Antarctic continent, associated with bottom water formation in the model. However, since the model does not allow for sea ice formation the details cannot be expected to be very realistic.

The model just discussed represents the ocean through a network (or "grid") of data points of between 200 km and 300 km separation. It is therefore unable to resolve the quasigeostrophic eddies which are so ubiquitous in the ocean and in some regions (particularly in the Southern Ocean; see Chapter 6) essential for the transport of heat and salt. Other models which use the most powerful computers presently available use grid representations with mesh sizes as small as 15 km. While we cannot expect these models to reproduce actually observed eddies in size, location, or life span, we can hope that the models reproduce the eddy statistics such as the distribution of eddy kinetic energy (Figure 17.10) and improve our estimates of oceanic heat flux by identifying the relative importance of eddy heat transport in different regions of the world ocean.

SST-based positive feedbacks in the tropical atmosphere

The recourse to a numerical model in the last section completes our discussion of the importance of the sea surface temperature as the coupling agent between ocean and atmosphere for establishing the mean climate. However, sea surface temperature provides the coupling agent on shorter time scales as well, and in the tropics its role for controlling the seasonal cycle is so important that a discussion of the mean climate would be incomplete without consideration of the mean seasonal cycle for the tropics. This also offers a natural introduction to the topic of the next chapter, variations in the seasonal cycle, or interannual variability.

Two prominent features of the atmospheric circulation over the Pacific Ocean are the Intertropical Convergence Zone (ITCZ) and the South Pacific Convergence Zone (SPCZ), which are seen as cloud bands in satellite imagery (Figs. 8.5 and 19.7). They are nearly always located near ridges of high SST, with temperatures of 28°C and above. The clouds are formed when moist near-surface air, transported equatorward and westward by the Trade Winds of both hemispheres, enters the Convergence Zones. The air then rises; moisture condenses into clouds, and intense rainfall occurs in the Convergence Zones (compare Figure 1.7). The condensation process releases huge amounts of latent heat into the surrounding air, which makes the air expand and keep on rising, thereby sucking more moist air in behind it. After reaching the top of the troposphere the warmed, dried air spreads sideways, loses its heat by radiative loss to space, and sinks back towards the sea surface (Figure 1.1), where the Trade Wind cycle begins again.

There are analogues of the ITCZ in the Indian Ocean region, associated with the Asian and Australian monsoons, and also over Africa and South America; but unlike the Pacific convection bands, the locations of these systems are to some extent set by geographic features (the Himalayas and the Andes).

The atmospheric convection cells of the tropics are the most energetic features of the global climate. They compete vigorously with one another, in the sense that a mature convection zone creates wind shears between upper level outflows and near-surface inflows for thousands of kilometers around it, and these shears strongly inhibit the formation of other convection zones. Competition between the two hemispheres produces a strong seasonal cycle, and the mechanism of the SST coupling introduces strong positive feedback, i.e. a tendency for instability, into the world's climate.

This is particularly noticeable each May - June when solar heating in the northern hemisphere starts to favour convection there at the expense of the southern hemisphere. At this time of year (and no other) SST increases to 29°C over most of the tropical Indian Ocean, and a store of moist air builds up over this region. By analogy with the Pacific ITCZ and SPCZ one might expect rainfall to develop over this SST maximum. However, this does not happen, most likely because convection over the Indian Ocean is being suppressed by the southern hemisphere convective systems of the Pacific Ocean. Whether for this or some other reason, convection over the Indian Ocean is weakening south of the equator, and some time around early June convection starts over Asia. The supply of very moist oceanic air is drawn towards the new convection centre which grows very rapidly; the SPCZ weakens rapidly at the same time - one might say that it can no longer compete. As a result of these developments the onset of the Indian summer monsoon is a dramatic and sudden event. For reasons not yet fully understood the onset of the Australian monsoon

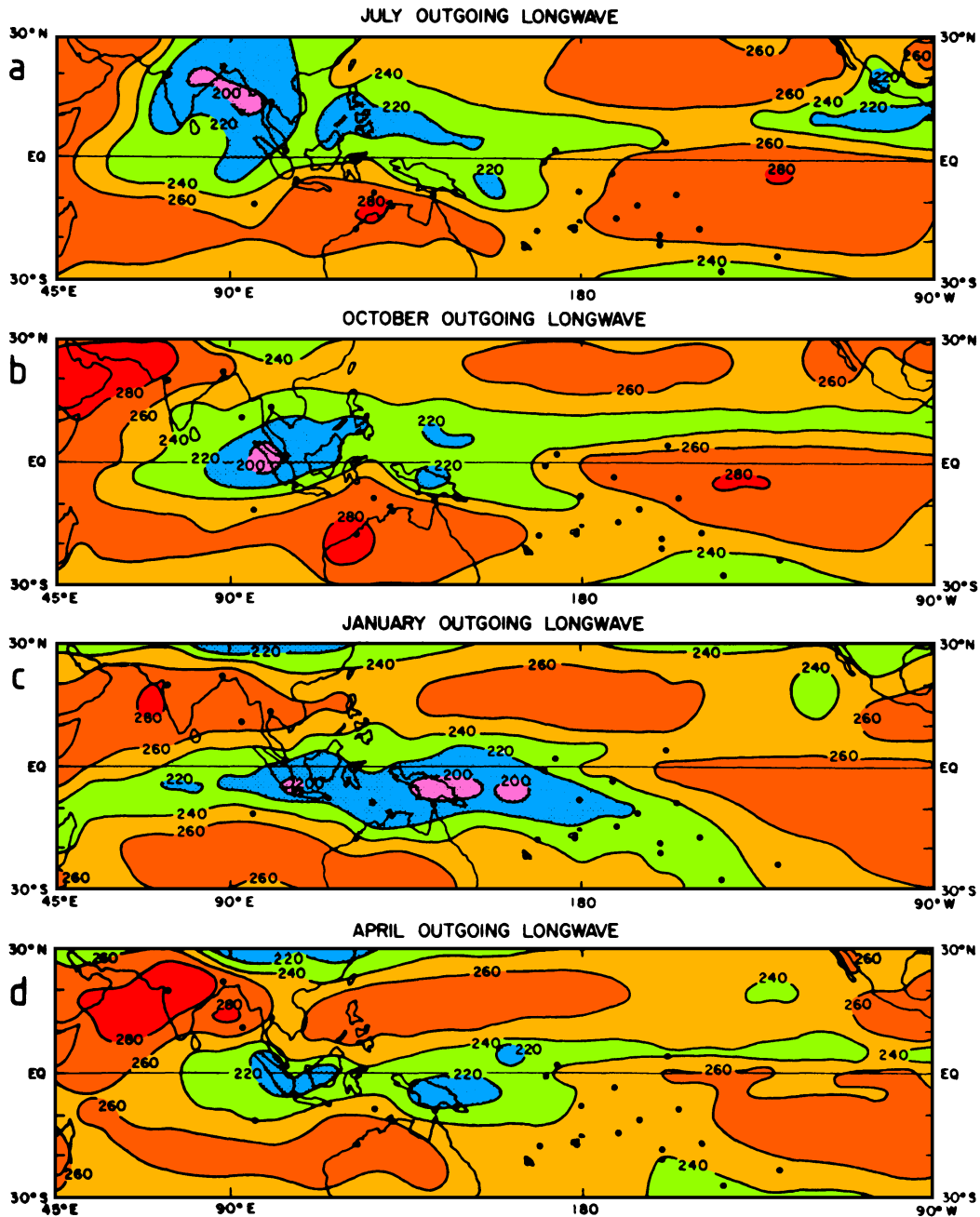


Fig.18.7. Long-term mean of outgoing longwave radiation (OLR, $W m^{-2}$) for the period June 1974 - November 1983 but excluding 1978, for the Indian and Pacific sectors. (a) July, (b) October, (c) January, (d) April. Areas of less than $220 W m^{-2}$ OLR are stippled, indicating greatest tropical convection. Adapted from Janowiak *et al.* (1985).

around November each year is not quite so dramatic; though it can be marked by rainfall that starts within one or two days over a longitude span of about 40° across northern Australia.

The clouds associated with the centres of rainfall (which are the driving force for these atmospheric circulations) influence the longwave back-radiation of incoming solar energy. Large cumulus towers in high rainfall areas reach very high and have very cold tops; they emit very little heat energy and are therefore seen in maps of outgoing longwave radiation (OLR) as local minima. Seasonal patterns of rainfall can therefore be followed by monitoring OLR from satellites. The observations reveal a prominent difference in the rainfall patterns of October and May (Figure 18.7). Convection crosses the equator rather smoothly in October, following the Indonesian Archipelago from Asia to Australia; while in April/May, just before the onset of the Asian summer monsoon, the convection is weak and split between Indonesia and the west Pacific Ocean. This hysteresis or asymmetry in the mean seasonal pattern of the atmospheric convection has the consequence that the biggest interannual changes in the earth's climate system tend to occur in May. The atmospheric circulation is very delicately poised at this time of year, and small changes in SST — and hence of moisture content in the atmosphere — can have disproportionately large effects on the atmospheric circulation. We explore this further in the following chapter.

